



PPI/CNT nanocomposite for novel high capacity removal of the toxic heavy metals, Hg, Pb and Ni from water

Bagher Hayati^a, Afshin Maleki^{a,*}, Farhood Najafi^b, Reza Rezaee^a, Shivaraju Harikaranahalli Puttaiah^c, Nader Marzban^d, Gordon McKay^{e,*}

^aEnvironmental Health Research Center, Research Institute for Health Development, Kurdistan University of Medical Sciences, Sanandaj, Iran,

^bDepartment of Environmental Research, Institute for Color Science and Technology Tehran, Tehran, Iran

^cDepartment of Water and Health, Faculty of Life Sciences, Jagadguru Sri Shivarathreeshwara University, Sri Shivarathreeshwara Nagara, Mysuru-570015, Karnataka, India

^dLeibniz Institute for Agricultural Engineering and Bioeconomy, Max-Eyth-Allee 100, 14469 Potsdam-Bornim, Germany

^eDivision of Sustainable Development, College of Science and Engineering, Hamad Bin Khalifa University, Education City, Qatar Foundation, Doha, Qatar, email: gmckay@qf.org.qa (G. McKay)

Received 25 September 2019; Accepted 6 May 2020

ABSTRACT

In this study, a new methodology is reported for the preparation of polypropylene imine dendrimer functionalized carbon nanotubes and a PPI/CNT nanocomposite. The PPI/CNT nanocomposite was characterized by Fourier-transform infrared spectroscopy, scanning electron microscopy, transmission electron microscopy, Raman spectroscopy, Brunauer–Emmett–Teller surface area and thermogravimetric analysis and this product has been applied to water pollution treatment for heavy metal removal and found to possess uniquely high adsorption capacities for Hg(II), Pb(II) and Ni(II). The effects of various parameters such as initial metal ion concentration, solution pH, PPI/CNT dosage and contact time have been studied. The data were analyzed by equilibrium isotherm relationships (Langmuir and Freundlich) and the exceptional high adsorption capacities (Hg = 2,000 mg/g; Pb = 1,750 mg/g; Ni = 1,650 mg/g) and adsorption rates were correlated by the pseudo-first-order, intraparticle diffusion and pseudo-second-order adsorption kinetics models. The results showed that the maximum adsorption occurred at pH = 7 and that the Langmuir isotherm and pseudo-second-order kinetics are the most favorable models for Hg(II), Pb(II) and Ni(II) ions adsorption onto PPI/CNT.

Keywords: PPI/CNT Nanocomposite; Novel synthesis route; Heavy metal ion adsorption; Kinetics and isotherm studies; Super-high capacities

1. Introduction

Heavy metal contamination in water systems is one of the most important ecosystem problems over the last few decades. Many tonnes of toxic metals including arsenic, cadmium, chromium, copper, mercury, nickel, lead, selenium and zinc are released from mining and industrial activities and are discharged into the environment

affecting public health and environmental systems particularly waterways [1] and soil [2]. Poisonous heavy metals are of specific concern in the purification of industrial wastewaters, these metals include chromium, nickel, lead, and mercury. Mercury is one of the most toxic elements, capable of drastically damaging the central nervous tissues; large concentrations of mercury create disorderliness in the kidney function and pulmonary, dyspnea and chest pains.

* Corresponding authors.

Lead can also harm the liver, kidney and reproductive function, fundamental cellular activities, and the brain system. A nickel contaminated environment has the potential to create various pathological effects including, lung fibrosis, cancer of the respiratory system and skin sensitivities [3]. Due to their great solubility in aqueous solutions, these toxic heavy metals can be simply absorbed by organisms and when they have arrived in the food chain and can accumulate in the human tissues, creating serious health disturbances [4]. The elimination and regeneration of heavy metal ions from industrial wastewaters can be attained by various techniques including coagulation, chemical precipitation, reduction, solvent extraction, electrochemical treatment, membrane separation, neutralization, ion exchange and adsorption processes [5]. Most of these techniques have a number of disadvantages, for example, incomplete removal, the output of toxic sludge and high energy expenditure [6]. From these methods, adsorption is suggested as one of the most efficient and economical techniques for the uptake of heavy metal ions. Many adsorbents have been used for metal ions from water and wastewater such as activated carbon, industrial solid wastes, clay minerals, zeolites and even orange peel [6].

Dendrimers possess a wide range of potential uses due to their excellent and tunable physical and chemical attributes. Initial applications were focused on their drug delivery characteristics [7,8] and for the removal of dyes from textile effluents [9,10]. Linking terminal groups, for example, carboxyl, amine, and hydroxyl as functional groups of dendrimers can lead to a considerable increase in the adsorptive capacity for the different metal ions [11]. These specific properties make dendrimers efficient and promising adsorbents in particular with respect to heavy metals removal [12,13]. Anbia and Haqshenas [14] prepared triazine dendrimers to adsorb Ni(II), Cu(II) and Zn (II). Zhao et al. [15] demonstrated Cu(II) and Pb(II) removal onto mesoporous carbon modified with amino-terminated dendrimer. Zhao and Xu [16] prepared a PAMAM dendrimer grafted to cellulose nanofibril for chromium adsorption. Diallo et al. [17] reported different generations of PAMAM dendrimers with amino-terminal groups for Cu(II) removal. Chaudhary et al. [18] studied Cu(II) removal by PAMAM dendrimers with amino functional groups. Cu(II) adsorption capacities of the PAMAM dendrimers were higher than those of linear polymeric adsorbents with amino groups.

From the many adsorbents, carbon nanotubes (CNT) have exhibited an inimitable impact on the rapid adsorption of dangerous materials from aqueous solutions, and because of their unparalleled chemical, physical and mechanical attributes [19], these nanostructured adsorbents have been applied for the uptake heavy metals from wastewaters [20]. The adsorption performance of CNTs can be improved by surface modification methods, which can permit the incorporation of appropriate functional groups capable to raise their dispersibility in the liquid phase to provide the nanoscale materials with strong chelating potential towards toxic heavy metal ions [21]. In addition, modified carbon nanotubes have the ability to be subjected to metal regeneration by desorption treatment as a function of the pH of the aqueous solution [22]. The established adsorption mechanism for carbon nanotubes is based on

chelation by covalent and non-covalent bonding. However, there is a lack of selectivity for heavy metal ions removal since these pollutants are frequently found in the presence of innocuous ions in water. Thus, there is a need for the continued exploration of surface modification techniques in the synthesis of CNTs with high adsorption efficiency for the toxic metal ions without competition for adsorption sites from innocuous ions is required [23]. In the search for selective chelating adsorbents, the monodisperse and hyper-branched dendrimers, containing functional amino groups, have exhibited a high chelating potential for toxic heavy metal ions adsorption [24]. The successful and high capacity removal of aromatics [25] and oil [26] from water has been investigated.

In this research, in addition to providing a new super adsorbent to remove heavy metal contamination from industrial wastewaters, we synthesized CNT with a PPI dendrimer as the chelating agent. Therefore, the aim of this study is to investigate the applicability of this PPI/CNT adsorbent to remove Hg(II), Pb(II) and Ni(II) in a batch system. The effect of several process parameters such as adsorbent dosage, initial metal ion concentration, solution pH, contact time and temperature have been investigated. In addition, the experimental data were correlated by using several isotherms and kinetics models and the adsorption thermodynamic parameters were determined to identify the nature of the sorption process.

2. Experimental setup

2.1. Material

Oxidized multi-walled carbon nanotubes (MWCNT-COOH) with an average size of 20–40 nm were obtained from Neutrino Company (Tehran, Iran). Ethylenediamine and acrylonitrile were obtained by Merck. Standard solutions of Hg(II), Pb(II) and Ni(II) (1,000 mg/L) were provided as the sulfate salts and the solution pH was regulated by adding the correct volumes of 0.02 M sulfuric acid and sodium hydroxide solutions. The other materials and reagents applied in this research were provided by Merck and Sigma-Aldrich Companies.

2.2. Synthesis of PPI dendrimer

A quantity of 4.4 g acrylonitrile was added to an aqueous solution of ethylenediamine (10.33 g/L). The exothermic process caused the temperature to increase to 40°C. Then, the mixture was heated at 85°C for 2 h to complete the reaction. The surplus of acrylonitrile was then removed as a water azeotrope by vacuum extraction (temperature 50°C and 18 mbar). The received crystalline solid was the half-generation of PPI dendrimer. In order to convert this half to the full generation PPI dendrimer, hydrogenation was performed. The half-generation PPI dendrimer, dissolved in methanol, was added to the hydrogenation container, and then Raney Nickel was added after pretreatment with hydroxide and distilled water. This mixture was then hydrogenated at 75°C and 30 atm hydrogen pressure for 3 h. The chilled reaction mixture was filtered and the organic solvents were vaporized at decreased pressure. The remaining solid was the

first generation of PPI dendrimers. PPI dendrimers up to four generations (32 surface amino groups) were synthesized by the repetition of all the above stages continuously, by adding surplus amounts of acrylonitrile (Fig. 1) [27].

2.3. Synthesis of PPI/CNT nanocomposite

PPI/CNTs were synthesized by amidation of MWCNT-COOH through two reaction stages. The acylation reaction was carried out by adding 10 g MWCNT-COOH into the blend of 10 mL N,N-dimethylformamide (DMF) and 200 mL thionyl chloride (SOCl₂) and heating it up to 75°C for 18 h with mechanical stirring. Then, the blend was chilled and rinsed with waterless tetrahydrofuran (THF) under nitrogen gas until the supernatant liquid was clear. Then the surface-acylated carbon nanotubes were dried at room temperature for the next application. For the preparation of PPI-functionalized CNTs, 8 g surface-acylated carbon nanotubes were mixed with 200 mL PPI dendrimer in a flask and heated under reflux at 100°C for 48 h. After chilling to room temperature, the surplus PPI was removed by suction and the black powder was washed three times using clear waterless THF to take up the adsorbed PPI on the surface of the CNTs. After drying at 80°C under vacuum, the PPI/CNT was obtained [28].

2.4. Characterization

Fourier-transform infrared (FTIR) spectra were determined using the KBr disk technique in the range of 400–4,000 cm⁻¹ by a Perkin-Elmer spectrophotometer. Zeta-potential values of the pristine and the functionalized MWCNTs were measured by using a Zeta sizer Nano ZS system (Malvern, UK) equipped with a standard 633 nm laser. The surface morphology of the CNTs and PPI/CNT nanocomposites were studied using a scanning electron microscope (Philips) at 20 kV after covering the nanoparticles with gold film. Transmission electron microscopy (TEM) analysis was carried out by the JEM-1200 EXII transmission

electron microscope. For this purpose one drop of nano-composite was put on copper lace coated with carbon and dried at 25°C [29]. Nuclear magnetic resonance (¹H NMR) studies were operated by a Varian Mercury Plus 500 MHz spectrometer using D₂O as the solvent.

2.5. Adsorption measurements

Inductively coupled plasma (ICP, Optima 2000 DV) was applied for measuring the metal ions concentrations in the sample solutions. The mass of metal ions removed per g dendrimer at equilibrium was calculated as follows [30]:

$$q_e = \frac{(C_0 - C_e)V}{m} \quad (1)$$

where q_e is the mass of metal ions adsorbed per gram of PPI/CNT at equilibrium and C_e and C_0 are the equilibrium and initial concentrations of metal ions in the liquid phase (mg/L) respectively. V is the volume solution including heavy metal ions (L) and m is the mass of PPI/CNT (g).

3. Results and discussion

3.1. Characterization of PPI/CNT nanocomposites

The functional groups available in the PPI modified CNT (PPI/CNT) were characterized by FTIR spectroscopy (Fig. 2). In the large frequency zone, a flattened band near 3,423 cm⁻¹ appeared in all spectra diagrams, which can be assigned to the stretching vibrations of hydroxyl (OH) groups in CNT or amino groups (NH₂) of the PPI. Absorption peaks around 2,917 and 2,852 cm⁻¹ in all the curves can be attributed to the aliphatic C–H stretching vibrations, the intensity of which is higher in PPI/CNT rather than the oxidized CNT. The peaks of C=O and C–O in oxidized CNT are observed at 1,708 and 1,246 cm⁻¹, respectively, which confirms the existence of carboxyl groups in CNT-COOH.

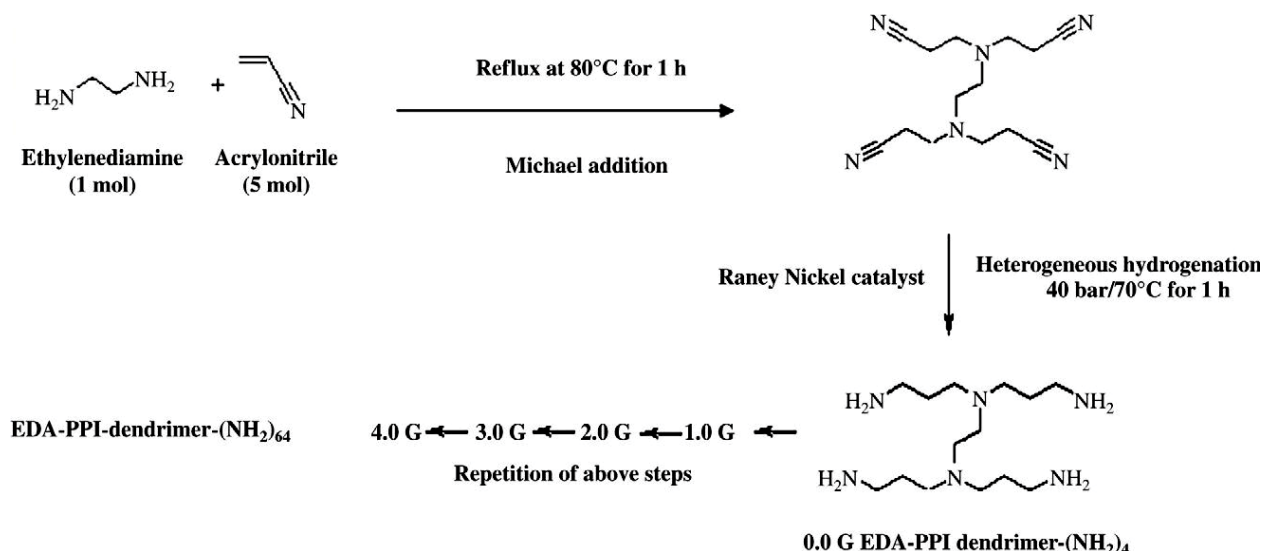


Fig. 1. Synthesis of the four generations of PPI dendrimer.

The peak around $1,673\text{ cm}^{-1}$ corresponds to the amide and the peak observed at $1,213$ is assigned to the amino group demonstrating that PPI dendrimers have been successfully

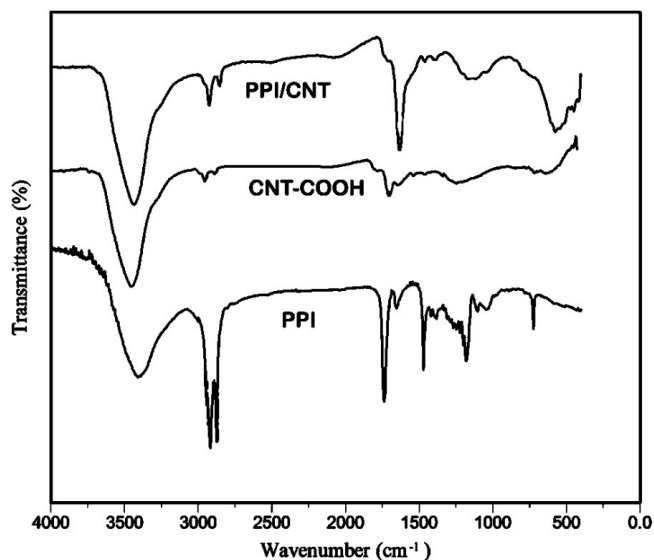


Fig. 2. FTIR spectra of CNT-COOH, PPI and PPI/CNT.

grafted to the oxidized CNT via the formation of amide groups [31].

Fig. 3 represents the surface specifications and morphologies of CNT-COOH and PPI/CNT via scanning electron microscopy (SEM) and TEM analysis. As observed in the images, the carbon nanotube's morphologies were undamaged after the amino functionalization treatments. The CNTs are stable enough to tolerate the oxidation pretreatment and grafting of PPI dendrimers. The CNT's surfaces were grafted with a small aggregation of PPI, which is equally divided along the carbon nanotubes. It is envisaged that PPI/CNTs are agglomerated leading to a sectional loss of monodispersity due to the high viscosity of PPI. These SEM analysis images indicate that PPI dendrimers were successfully grafted onto the surface of CNTs [32].

The pore size and specific surface areas of CNT-COOH and PPI/CNT were studied by nitrogen adsorption/desorption measurements at 84 K. The samples indicated a type 2 isotherm, ascribed to the porosity structure of CNTs. It is expected that the CNTs are a desirable substrate material for PPI grafting because of their physical stability and large pore sizes. Table 1 represents the surface properties of the synthesis materials including specific surface area (S_{BET} , m^2/g), total pore volume estimated (V_{total} , cm^3/g), mesopore volume, which was determined from the BJH equation (V_{Meso} , cm^3/g) and micropore volume determined from the

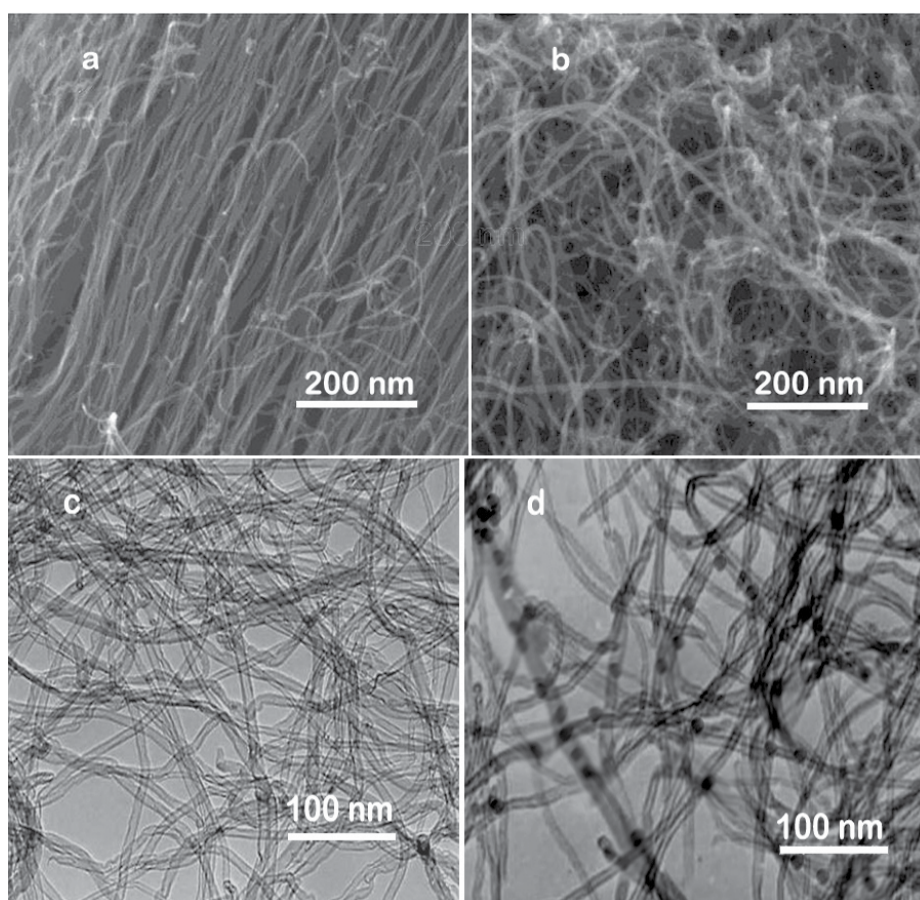


Fig. 3. SEM images of (a) CNT-COOH, (b) PPI/CNT and TEM images of (c) CNT-COOH, and (d) PPI/CNT.

Table 1
Surface properties of CNT-COOH, PPI and PPI/CNT

Samples	CNT-COOH	PPI/CNT
S_{BET} (m^2/g)	387	343
V_{total} (cm^3/g)	2.458	1.762
V_{Meso} (cm^3/g)	2.431	1.746
V_{Micro} (cm^3/g)	0.027	0.016

subtraction of mesopore volume from total pore volume. CNTs have a large specific surface area and pore volume. The pore volume and specific surface area are reduced after grafting the PPI onto the CNTs, indicating that the nitrogen molecules could not pass through the pore entrances due to the obstruction caused by the amino groups of the PPI dendrimers [33].

Raman analysis of the CNT-COOH and PPI/CNT showed two specific peaks; one at $1,315 \text{ cm}^{-1}$ because of the D-band and the second peak because of the G-band at $1,587 \text{ cm}^{-1}$ (Fig. 4). The G-band for CNTs is ascribed to the inherent vibrations of sp^3 linked graphitic bond among carbon atoms whereas the D-band is attributed to the deficiencies induced in the carbon nanotubes because of the rupture of sp^2 alkene (C=C) bonds. The intensity of the G-band of PPI/CNT was slightly decreased rather than in the case of CNT-COOH because of the reduction in impurities on the CNTs after grafting by PPI dendrimers. In this study, a larger $I_{\text{D}}/I_{\text{G}}$ quantity indicates a larger disruption of the sp^2 bonded carbon atoms to sp^3 hybridized carbon atoms, demonstrating that a higher degree of covalent bond has appeared on the surfaces of the oxidized carbon nanotubes. In addition, the $I_{\text{D}}/I_{\text{G}}$ value of PPI/CNT specimen ($I_{\text{D}}/I_{\text{G}} = 0.68$) is more than that for oxidized CNTs ($I_{\text{D}}/I_{\text{G}} = 0.46$), promising that the PPI dendrimers are covalently linked onto the surfaces of CNTs [34].

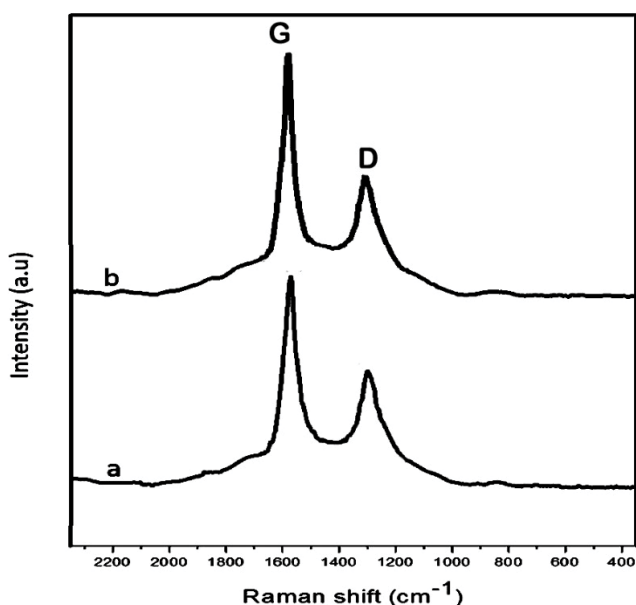


Fig. 4. Raman spectra of CNT-COOH and PPI/CNT.

The thermal gravimetric analyses of CNT-COOH and PPI/CNT are shown in Fig. 5. In CNT-COOH, the first stage of weight loss can be observed between 65°C and 230°C indicating there is a 14.8% weight loss, assigned to the removal of adsorbed water and the decomposition of labile oxygen functional groups. Then, a sharp second weight loss (18%) occurs from 410°C to 594°C , which can be attributed to the decomposition of the oxygen or functional groups. The first weight loss of PPI/CNT was observed between 71°C and 311°C (62%) and which is attributed to the decomposition of oxygen and nitrogen components then, an abrupt weight loss (11%) occurs from 311°C to 800°C . As shown in Fig. 5, the thermal stability of CNT-COOH is better than that of PPI/CNT [35].

3.2. Effective parameters on the sorption process

3.2.1. Effect of pH

pH is the main factor that highly affects the heavy metals removal because the solution pH can affect not only the ionic strength but also the total charge of the sorbent. The effect of pH on the adsorption capacity of Hg(II), Pb(II) and Ni(II) has been performed by a series of metal ion solutions with different pH values (2–7). As shown in Fig. 6, the sorption capacity is enhanced by increasing the pH from 2 to 7. This removal trend is probably affected by the electrostatic repulsion among positive amino groups on PPI/CNT and the positive charge of metal ions Hg(II), Pb(II) and Ni(II) can bind with amino groups of PPI/CNT via the coordination bond with the nitrogen lone pair of electrons. At low pH, the electrostatic repulsion is strong as some NH_2 groups are protonated to $-\text{NH}_3^+$ thus repelling the positive metal ions. Therefore, the removal capacity at acidic pH is less than that at neutral pH. In these experiments, all three metal ions started to precipitate at $\text{pH} > 7$. The Hg(II), Pb(II) and Ni(II) ions do not precipitate in solution at $\text{pH} = 7$, therefore, this pH is selected as an optimum [36].

3.2.2. Effect of adsorbent dosage

The quantity of sorbent in the liquid phase is one of the important factors in the sorption process. As shown in Fig. 7, the effect of PPI/CNT dosage on the adsorption was

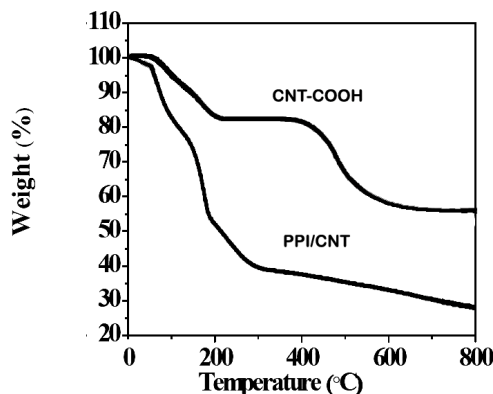


Fig. 5. Thermogravimetric analysis of CNT-COOH and PPI/CNT.

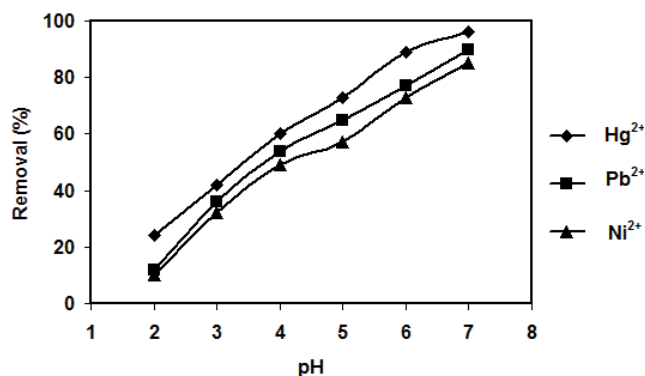


Fig. 6. Effect of pH on heavy metal adsorption by PPI/CNT ($C_0 = 100$ mg/L; $C_{\text{sorbent}} = 0.06$ g/L; $T = 298$ K).

investigated when the initial metal ion concentration was 100 mg/L at 25°C, the pH was 7 and the contact time was 10 min. Under a given Hg(II), Pb(II) and Ni(II) metal ion concentration, the PPI/CNT would be used practically with a low dose and usage of unit mass sorbent is modified, while the uptake percentage of metal ions may be unsatisfactory according to environmental legislation. Increasing the quantities of PPI/CNT can improve the uptake amount of metal ion because of the increased number of the sorption sites but the specific metal ion uptake capacity is decreased. Therefore, regarding the adsorption amount of metal ion and the consumption rate of PPI/CNT, the optimal amount of adsorbent dose was selected [36].

3.2.3. Effect of contact time and initial metal ion concentration

Fig. 8 shows the effect of contact time on the amount of PPI/CNT sorbent for Hg(II), Pb(II) and Ni(II) removal from aqueous solutions with several initial metal ion concentrations of 50, 100, 150, 200 mg/L at 25°C. The sorption capacity of all three metal ions was enhanced sharply with adsorption contact time in the first 10 min and the contact time to reach equilibrium capacity state was 20 min. It is also obvious from Fig. 8 that the efficiency of removal increased with an increase in the initial concentration of metal ions, and then the initial concentrations of metal ions had no considerable effect on the saturation time. The increase in the removal capacity is because of the higher interaction between the adsorbent and adsorbate. Filling up more of the free or “available” $-\text{NH}_2$ sites on the adsorbent [36].

3.3. Adsorption kinetics

The adsorption kinetics were studied to explain the rate of heavy metal ion adsorption and to investigate the mechanism of metal ion removal controlling the sorption rate. These empirical data were characterized and calculated using three kinetic models comprising the pseudo-first-order, intra-particle diffusion and pseudo-second-order equations [37,38].

The pseudo-first-order equation [Eq. (2)] and the pseudo-second-order equation [Eq. (3)] kinetics were applied to

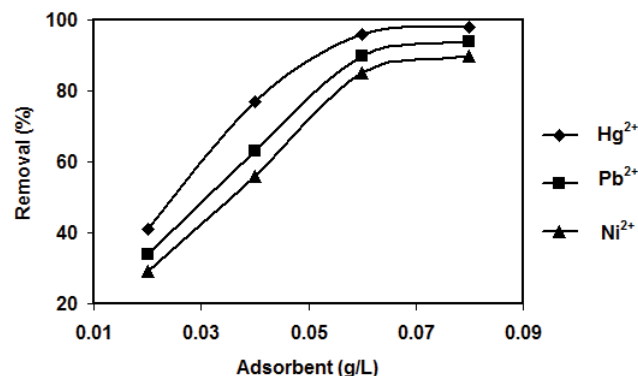


Fig. 7. Effect of the sorbent dose on heavy metal removal by PPI/CNT ($C_0 = 100$ mg/L; pH = 7; $T = 298$ K).

assess the rate constant and to describe the mechanism of the sorption procedure. Their linear forms [39] can be represented by Eqs. (2) and (3):

Pseudo-first-order:

$$\log(q_e - q_t) = \log q_e - \frac{k_1}{2.303t} \quad (2)$$

Pseudo-second-order:

$$\frac{t}{q_t} = \frac{1}{k_2 q_e^2} + \frac{1}{q_e} t \quad (3)$$

where q_e (mg/g) is the sorption capacity of PPI/CNT nanocomposite in equilibrium saturation state; k_1 (1/min) is the velocity constant of the pseudo-first-order kinetic model; and k_2 (g/mg min) is the velocity constant of the pseudo-second-order kinetic model. The kinetic parameters obtained are represented in Table 2. For Hg(II), Pb(II) and Ni(II) metal ions removal by PPI/CNT, computed correlation coefficients (R^2) are closer to the pseudo-second-order kinetic model ($R^2 = 0.999$) compared with the pseudo-first-order kinetic model. Moreover, the theoretical q_e computed from the pseudo-second-order equation fitted well to the experimental equilibrium quantities of adsorbed Hg(II), Pb(II) and Ni(II) metal ions (q_{exp}) in Table 2. Thus, these findings demonstrated that the metal ion adsorption by PPI/CNT nanocomposite agreed very well with the pseudo-second-order model [40].

The intra-particle diffusion model [Eq. (4)] was also applied to further investigate the mechanism of PPI/CNT nanocomposite for Hg(II), Pb(II) and Ni(II) metal ions removal by considering the diffusion of the metal ions [41].

$$q_t = k_p t^{1/2} + I \quad (4)$$

where k_p is the intra-particle diffusion constant (mg/g min) and I is a constant relevant to the range of the external boundary layer effect. The kinetic parameters of PPI/CNT nanocomposite are represented in Table 2. The R^2 values of Hg(II), Pb(II) and Ni(II) metal ions are less than 0.7, which illustrates that intra-particle diffusion had no significant role

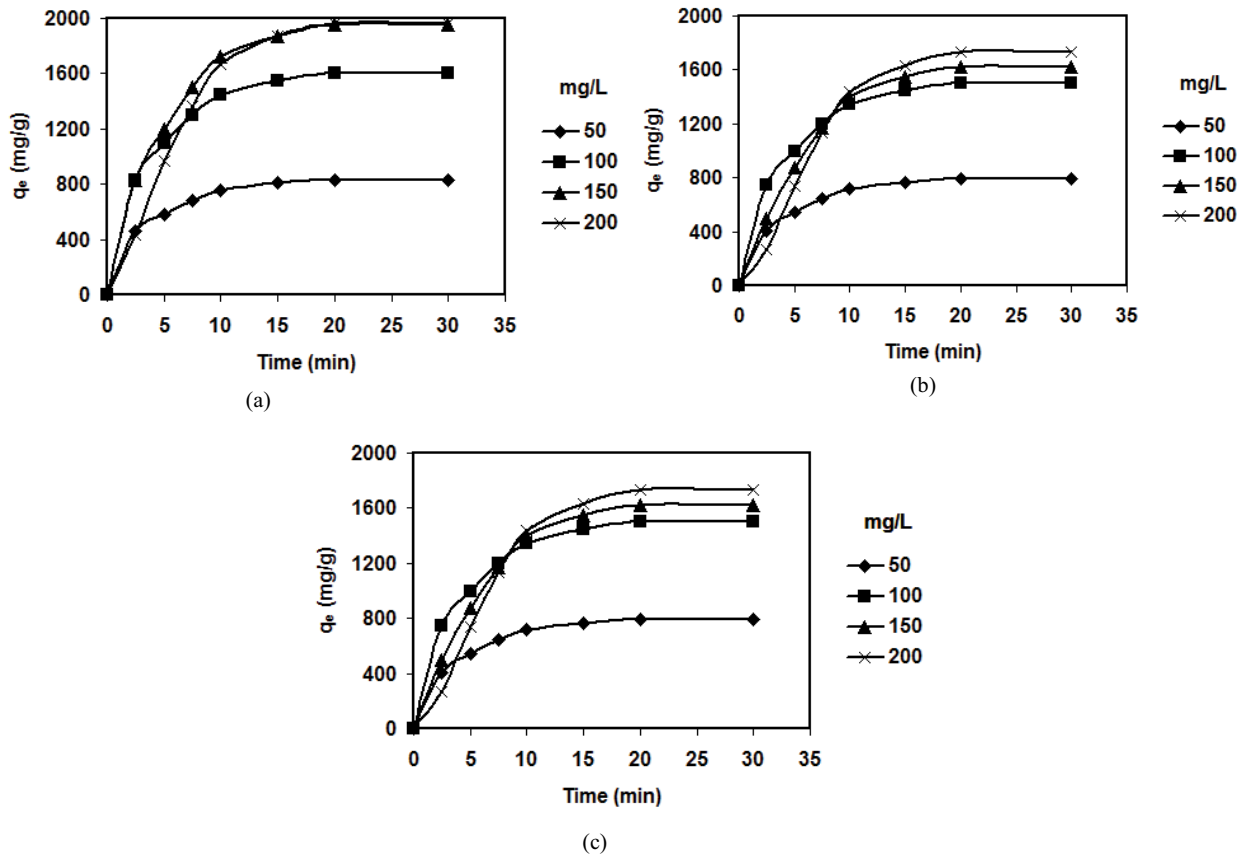


Fig. 8. Effect of initial metal concentration and contact time on (a) Hg(II), (b) Pb(II), and (c) Ni(II) ions removal by PPI/CNT (pH = 7; $C_{adsorbent} = 0.06$ g/L; $T = 25^{\circ}\text{C}$).

Table 2
Kinetic parameters of heavy metal adsorption on PPI/CNT (pH = 7; $C_{adsorbent} = 0.06$ g/L; $T = 298$ K)

Metals (100 mg/L)	q_{exp}	Pseudo-first-order			Pseudo-second-order			Intraparticle diffusion		
		q_{ecal}	k_1	R^2	q_{ecal}	k_2	R^2	k_p	I	R^2
Hg(II)	2,000	3,345	0.413	0.885	1,850	0.019	0.999	403	869	0.676
Pb(II)	1,750	2,975	0.437	0.891	1,650	0.031	0.999	379	721	0.700
Ni(II)	1,650	2,247	0.465	0.899	1,450	0.047	0.999	318	593	0.692

in the adsorption process [42]. The very short time (20 min) to achieve equilibrium also suggests a surface complexation–chelation mechanism rather than an internal diffusion mechanism.

3.4. Adsorption isotherm

Adsorption isotherm models provide a quantitative assessment on the nature of the surface interaction and also the special relevance between the concentration of polluting ions and its amount of agglomeration onto the adsorbent surface at a fixed temperature [43,44]. The adsorption isotherms are important in optimizing the application of the adsorbents, and the evaluation of the isotherm data by correlating them to various isotherm equations is a major step to select the appropriate model that can be applied for

estimating the capacity of a wastewater treatment plant. In this research, the Langmuir, Freundlich and Temkin isotherm equations were employed to evaluate the relationship between the adsorbed Hg(II), Pb(II) and Ni(II) metal ions removal onto PPI/CNT nanocomposite.

The Langmuir isotherm [45,46] considers that a solid surface has a limited number of equal sites that exhibit homogeneous adsorption behavior. The linearized form of the Langmuir model is represented by Eq. (5):

$$\frac{C_e}{q_e} = \frac{1}{K_L Q_0} + \frac{C_e}{Q_0} \tag{5}$$

where q_e (mg/g) is the amount of metal ion adsorbed per one weight of the PPI/CNT at equilibrium, C_e (g/L) is

Table 3

Isotherm parameters of heavy metal adsorption on PPI/CNT (pH = 7; $C_{\text{adsorbent}} = 0.06 \text{ g/L}$; $T = 298 \text{ K}$)

Metal	Langmuir isotherm				Freundlich isotherm		
	Q_0	K_L	R_L	R^2	K_F	n	R^2
Hg(II)	2,000	1.433	0.015	0.999	1,460	4.112	0.896
Pb(II)	1,750	1.347	0.021	0.999	1,258	3.650	0.943
Ni(II)	1,650	1.760	0.028	0.999	1,114	3.742	0.956

the saturation concentration of a metal ion in the liquid phases, Q_0 (mg/g) is the maximum adsorption capacity and K_L (dm^3/mg) is the Langmuir constant referred to as the free energy of the adsorption process. The isotherm constants Q_0 (mg/g) and K_L were computed from the slope and intercept of the linearized Langmuir plot of C_e/q_e against C_e [47]. The quantities of the adsorption capacity Q_0 , K_L and the correlation coefficient (R^2) are presented in Table 3. The values of the correlation coefficient indicate good agreement of the Langmuir model for the adsorption of Hg(II), Pb(II) and Ni(II) metal ions removal onto PPI/CNT nanocomposite.

The Freundlich equation also exhibits relatively good fittings to the adsorption of heavy metals but poorer than the Langmuir. The linear form of the Freundlich adsorption equation [27,48] is shown in Eq. (6):

$$\log q_e = \log K_F + \frac{1}{n} \log C_e \quad (6)$$

where q_e (mg/g) is the quantities of metal ions removed per unit weight of PPI/CNT, C_e (mg/L) is the equilibrium concentration of metal ions in the aqueous solution; K_F ($\text{mg/g})^{n/(n-1)}$ is the Freundlich constant, which is a relative measure of the adsorption capacity of the PPI/CNT and n is an experimental constant referred to the heterogeneity of the sorbent surface. The parameter n also demonstrates the nature of the adsorption process. If the amount of $1/n$ is in range of between 0 and 1, this model is favorable, while $n > 1$ represents favorable sorption, and $n = 1$ shows the linear equation, if $n = 0$, the adsorption operation is irreversible [1,49]. The isotherm constants n and K_F were computed from the slope and intercept of the plot $\log q_e$ against $\log C_e$. The values of the Freundlich constants and correlation coefficients (R^2) are presented in Table 3.

These capacities are exceptionally high when compared with more conventional adsorbents and ion exchangers. Even studies using ethylenediaminetetraacetic acid-functionalized graphene oxide nanoparticles [50] had a capacity of only 1 mg/g for mercury. For mercury removal, cheaper adsorbents, such as coal [51] and modified orange peel [52] had capacities of 2.82 and 38.4 mg mercury/g adsorbent respectively. For lead removal by perlite [53] a capacity of almost 18.5 mg/g was achieved [54]; and magnetic nanoparticles were capable of removing over 14.0 mg lead/g adsorbent. In the case of nickel, a lichen species [55] could adsorb 14.7 mg/g; using a tailor-made resin [56], an iminodiacetate chelating resin [57] could adsorb 400 mg lead/g and an aluminosilicate ion exchange resin [58] could adsorb 120 mg nickel/g. All these materials still have significantly lower

heavy metal removal capacities than the PPI/CNT nanocomposites reported in this paper.

4. Conclusion

In this work, the preparation, specification and heavy metal ion uptake of PPI/CNT as a high-performance adsorbent have been evaluated. PPI/CNTs were analyzed and characterized by FTIR, SEM, TEM, Raman spectra and thermogravimetric analysis methods. The removals of Hg(II), Pb(II) and Ni(II) metal ions have been studied as model pollutants. The results indicated that PPI/CNT has exceptionally high adsorption capacities for the Hg(II), Pb(II) and Ni(II) metal ions from the liquid phase. At neutral pH, the amount of negative charge is an important factor for the removal of metal ions. By increasing the PPI/CNT dosage, the adsorption performance constantly increased for three metal ions. This can be assigned to the increased adsorbent surface area and accessibility of many sorption sites. The findings also indicated that metal removal by PPI/CNT is a very rapid process thus resulting in short contact time for a wastewater treatment plant and so reducing capital costs by virtue of smaller equipment size requirements. Analysis of the sorption process indicated that the Langmuir isotherm and pseudo-second-order kinetics are appropriate equations for correlating Hg(II), Pb(II) and Ni(II) metal ions adsorption onto PPI/CNT. The Q_0 values in Table 3, Hg(II) 2,000 mg/g; Pb(II) 1,750 mg/g; Ni(II) 1,650 mg/g; demonstrate the tremendously high adsorption capacities of the PPI nanocomposite dendrimers.

Acknowledgement

This manuscript is extracted from the Ph.D. thesis of the first author and approved by the Environmental Health Research Center and funded by the Kurdistan University of Medical Sciences. The authors offer their thanks to the sponsors of the project.

References

- [1] B. Hayati, N.M. Mahmoodi, A. Maleki, Dendrimer–titania nanocomposite: synthesis and dye-removal capacity, *Res. Chem. Intermed.*, 41 (2015) 3743–3757.
- [2] A. Maleki, E. Pajootan, B. Hayati, Ethyl acrylate grafted chitosan for heavy metal removal from wastewater: equilibrium, kinetic and thermodynamic studies, *J. Taiwan Inst. Chem. Eng.*, 51 (2015) 127–134.
- [3] A. Maleki, B. Hayati, F. Najafi, F. Gharibi, S.W. Joo, Heavy metal adsorption from industrial wastewater by PAMAM/

- TiO₂ nanohybrid: preparation, characterization and adsorption studies, *J. Mol. Liq.*, 224 (2016) 95–104.
- [4] J. Wang, G. Zhao, Y. Li, H. Zhu, X. Peng, X. Gao, One-step fabrication of functionalized magnetic adsorbents with large surface area and their adsorption for dye and heavy metal ions, *Dalton Trans.*, 43 (2014) 11637–11645.
- [5] L. Mihaly-Cozmuta, A. Mihaly-Cozmuta, A. Peter, C. Nicula, H. Tutu, D. Silipas, E. Indrea, Adsorption of heavy metal cations by Na-clinoptilolite: equilibrium and selectivity studies, *J. Environ. Manage.*, 137 (2014) 69–80.
- [6] M. Xiao, J. Hu, Cellulose/chitosan composites prepared in ethylene diamine/potassium thiocyanate for adsorption of heavy metal ions, *Cellulose*, 24 (2017) 2545–2557.
- [7] D. Huang, D. Wu, Biodegradable dendrimers for drug delivery, *Mater. Sci. Eng., C*, 90 (2018) 713–727.
- [8] A. Siriviriyannun, Y.-J. Tsai, S.H. Voon, S.F. Kiew, T. Imae, L.V. Kiew, C.Y. Looi, W.F. Wong, H.B. Lee, L.Y. Chung, Cyclodextrin- and dendrimer-conjugated graphene oxide as a nanocarrier for the delivery of selected chemotherapeutic and photosensitizing agents, *Mater. Sci. Eng., C*, 89 (2018) 307–315.
- [9] N.M. Mahmoodi, B. Hayati, M. Arami, F. Mazaheri, Single and binary system dye removal from colored textile wastewater by a dendrimer as a polymeric nanoarchitecture: equilibrium and kinetics, *J. Chem. Eng. Data*, 55 (2010) 4660–4668.
- [10] B. Hayati, N.M. Mahmoodi, M. Arami, F. Mazaheri, Dye removal from colored textile wastewater by poly (propylene imine) dendrimer: operational parameters and isotherm studies, *Clean–Soil Air Water*, 39 (2011) 673–679.
- [11] M.R. Kotte, A.T. Kuvarega, M. Cho, B.B. Mamba, M.S. Diallo, Mixed matrix PVDF membranes with in situ synthesized PAMAM dendrimer-like particles: a new class of sorbents for Cu(II) recovery from aqueous solutions by ultrafiltration, *Environ. Sci. Technol.*, 49 (2015) 9431–9442.
- [12] M.S. Diallo, W. Arasho, J.H. Johnson Jr., W.A. Goddard III, Dendritic chelating agents. 2. U(VI) binding to poly (amidoamine) and poly(propyleneimine) dendrimers in aqueous solutions, *Environ. Sci. Technol.*, 42 (2008) 1572–1579.
- [13] A.N. Golikand, K. Didehban, L. Irannejad, Synthesis and characterization of triazine-based dendrimers and their application in metal ion adsorption, *J. Appl. Polym. Sci.*, 123 (2012) 1245–1251.
- [14] M. Anbia, M. Haqshenas, Adsorption studies of Pb(II) and Cu(II) ions on mesoporous carbon nitride functionalized with melamine-based dendrimer amine, *Int. J. Environ. Sci. Technol.*, 12 (2015) 2649–2664.
- [15] J. Zhao, X. Zhang, X. He, M. Xiao, W. Zhang, C. Lu, A super biosorbent from dendrimer poly (amidoamine)-grafted cellulose nanofibril aerogels for effective removal of Cr(VI), *J. Mater. Chem. A*, 3 (2015) 14703–14711.
- [16] Y. Xu, D. Zhao, Removal of copper from contaminated soil by use of poly (amidoamine) dendrimers, *Environ. Sci. Technol.*, 39 (2005) 2369–2375.
- [17] M.S. Diallo, S. Christie, P. Swaminathan, J.H. Johnson, W.A. Goddard, Dendrimer enhanced ultrafiltration. 1. Recovery of Cu(II) from aqueous solutions using PAMAM dendrimers with ethylene diamine core and terminal NH₂ groups, *Environ. Sci. Technol.*, 39 (2005) 1366–1377.
- [18] S. Chaudhary, A. Gothwal, I. Khan, S. Srivastava, R. Malik, U. Gupta, Polypropyleneimine and polyamidoamine dendrimer mediated enhanced solubilization of bortezomib: comparison and evaluation of mechanistic aspects by thermodynamics and molecular simulations, *Mater. Sci. Eng., C*, 72 (2017) 611–619.
- [19] B. Hayati, A. Maleki, F. Najafi, H. Daraei, F. Gharibi, G. McKay, Synthesis and characterization of PAMAM/CNT nanocomposite as a super-capacity adsorbent for heavy metal (Ni²⁺, Zn²⁺, As³⁺, Co²⁺) removal from wastewater, *J. Mol. Liq.*, 224 (2016) 1032–1040.
- [20] B. Hayati, A. Maleki, F. Najafi, H. Daraei, F. Gharibi, G. McKay, Adsorption of Pb²⁺, Ni²⁺, Cu²⁺, Co²⁺ metal ions from aqueous solution by PPI/SiO₂ as new high performance adsorbent: preparation, characterization, isotherm, kinetic, thermodynamic studies, *J. Mol. Liq.*, 237 (2017) 428–436.
- [21] B. Hayati, A. Maleki, F. Najafi, H. Daraei, F. Gharibi, G. McKay, Super high removal capacities of heavy metals (Pb²⁺ and Cu²⁺) using CNT dendrimer, *J. Hazard. Mater.*, 336 (2017) 146–157.
- [22] E.M. Elsehly, N.G. Chechenin, A.V. Makunin, H.A. Motaweh, E.A. Vorobyeva, K.A. Bukunov, E.G. Leksina, A.B. Priselkova, Characterization of functionalized multiwalled carbon nanotubes and application as an effective filter for heavy metal removal from aqueous solutions, *Chin. J. Chem. Eng.*, 24 (2016) 1695–1702.
- [23] P. Kesharwani, A. Gothwal, A.K. Iyer, K. Jain, M.K. Chourasia, U. Gupta, Dendrimer nanohybrid carrier systems: an expanding horizon for targeted drug and gene delivery, *Drug Discovery Today*, 23 (2018) 300–314.
- [24] R.S. Hebbar, A.M. Isloor, K. Ananda, A.F. Ismail, Fabrication of polydopamine functionalized halloysite nanotube/polyetherimide membranes for heavy metal removal, *J. Mater. Chem. A*, 4 (2016) 764–774.
- [25] R.S. DeFever, N.K. Geitner, P. Bhattacharya, F. Ding, P.C. Ke, S. Sarupria, PAMAM dendrimers and graphene: materials for removing aromatic contaminants from water, *Environ. Sci. Technol.*, 49 (2015) 4490–4497.
- [26] N.K. Geitner, B. Wang, R.E. Andorfer, D.A. Ladner, P.C. Ke, F. Ding, Structure–function relationship of PAMAM dendrimers as robust oil dispersants, *Environ. Sci. Technol.*, 48 (2014) 12868–12875.
- [27] N.K. Mehra, N.K. Jain, Multifunctional hybrid-carbon nanotubes: new horizon in drug delivery and targeting, *J. Drug Targeting*, 24 (2016) 294–308.
- [28] N.M. Mahmoodi, U. Sadeghi, A. Maleki, B. Hayati, F. Najafi, Synthesis of cationic polymeric adsorbent and dye removal isotherm, kinetic and thermodynamic, *J. Ind. Eng. Chem.*, 20 (2014) 2745–2753.
- [29] M. Yusuf, M.A. Khan, E.C. Abdullah, M. Elfgi, M. Hosomi, A. Terada, S. Riya, A. Ahmad, Dodecyl sulfate chain anchored mesoporous graphene: synthesis and application to sequester heavy metal ions from aqueous phase, *Chem. Eng. J.*, 304 (2016) 431–439.
- [30] A. Mohamed, S. Yousef, M.A. Abdelnaby, T.A. Osman, B. Hamawandi, M.S. Toprak, M. Muhammed, A. Uheida, Photocatalytic degradation of organic dyes and enhanced mechanical properties of PAN/CNTs composite nanofibers, *Sep. Purif. Technol.*, 182 (2017) 219–223.
- [31] X. Li, N. Xu, H. Li, M. Wang, L. Zhang, J. Qiao, 3D hollow sphere Co₃O₄/MnO₂-CNTs: its high-performance bi-functional cathode catalysis and application in rechargeable zinc-air battery, *Green Energy Environ.*, 2 (2017) 316–328.
- [32] M.U. Khan, K.R. Reddy, T. Snguanwongchai, E. Haque, V.G. Gomes, Polymer brush synthesis on surface modified carbon nanotubes via in situ emulsion polymerization, *Colloid. Polym. Sci.*, 294 (2016) 1599–1610.
- [33] Z.-Q. Duan, X.-B. Gao, T.-P. Li, K. Yao, X.-M. Xie, A facile route to the hierarchical assembly of Au nanoparticles on carbon nanotubes through Cu²⁺ coordination for surface-enhanced Raman scattering, *Chin. Chem. Lett.*, 28 (2017) 521–524.
- [34] M.A. Salam, A.Y. Obaid, R.M. El-Shishtawy, S.A. Mohamed, Synthesis of nanocomposites of polypyrrole/carbon nanotubes/silver nano particles and their application in water disinfection, *RSC Adv.*, 7 (2017) 16878–16884.
- [35] G. Zhou, J. Luo, C. Liu, L. Chu, J. Ma, Y. Tang, Z. Zeng, S. Luo, A highly efficient polyampholyte hydrogel sorbent based fixed-bed process for heavy metal removal in actual industrial effluent, *Water Res.*, 89 (2016) 151–160.
- [36] D.K. Yadav, S. Srivastava, Carbon nanotubes as adsorbent to remove heavy metal ion (Mn²⁺) in wastewater treatment, *Mater. Today: Proc.*, 4 (2017) 4089–4094.
- [37] S.U. Yoon, B. Mahanty, H.M. Ha, C.G. Kim, Phenol adsorption on surface-functionalized iron oxide nanoparticles: modeling of the kinetics, isotherm, and mechanism, *J. Nanopart. Res.*, 18 (2016) 1–10.
- [38] H. Rao, Z. Lu, W. Liu, Y. Wang, H. Ge, P. Zou, H. He, The adsorption of bone-related proteins on calcium phosphate ceramic particles with different phase composition and its adsorption kinetics, *Surf. Interface Anal.*, 48 (2016) 1048–1055.

- [39] L. Jia, X. Yao, J. Ma, C. Long, Adsorption kinetics of water vapor on hypercrosslinked polymeric adsorbent and its comparison with carbonaceous adsorbents, *Microporous Mesoporous Mater.*, 241 (2017) 178–184.
- [40] M. Rajabi, O. Moradi, K. Zare, Kinetics adsorption study of the ethidium bromide by graphene oxide as adsorbent from aqueous matrices, *Int. Nano Lett.*, 7 (2017) 35–41.
- [41] P.J. Vodanitskaia, J.J. Soares, H. Melo, J.M. Gurgel, Experimental chiller with silica gel: adsorption kinetics analysis and performance evaluation, *Energy Convers. Manage.*, 132 (2017) 172–179.
- [42] F. Ebadi Ahsan, M. Montazer, S.H. Amirshahi, M. Ghanbar Afjeh, T. Harifi, Influence of nano colloidal silver in dyeing of wool with acid blue 92: isotherm adsorption, kinetic studies and dyed wool characterization, *J. Nat. Fibers*, 13 (2016) 204–214.
- [43] N.M. Mahmoodi, B. Hayati, M. Arami, Textile dye removal from single and ternary systems using date stones: kinetic, isotherm, and thermodynamic studies, *J. Chem. Eng. Data*, 55 (2010) 4638–4649.
- [44] L.S. Chan, W.H. Cheung, S.J. Allen, G. McKay, Error analysis of adsorption isotherm models for acid dyes onto bamboo derived activated carbon, *Chin. J. Chem. Eng.*, 20 (2012) 535–542.
- [45] N.M. Mahmoodi, B. Hayati, H. Bahrami, M. Arami, Dye adsorption and desorption properties of mentha pulegium in single and binary systems, *J. Appl. Polym. Sci.*, 122 (2011) 1489–1499.
- [46] B. Hayati, N.M. Mahmoodi, Modification of activated carbon by the alkaline treatment to remove the dyes from wastewater: mechanism, isotherm and kinetic, *Desal. Water Treat.*, 47 (2012) 322–333.
- [47] B. Hayati, M. Arami, A. Maleki, E. Pajootan, Thermodynamic properties of dye removal from colored textile wastewater by poly(propylene imine) dendrimer, *Desal. Water Treat.*, 56 (2015) 97–106.
- [48] B. Erdem, M. Erdem, A.S. Özcan, Adsorption of reactive black 5 onto quaternized 2-dimethylaminoethyl methacrylate based polymer/clay nanocomposites, *Adsorption*, 22 (2016) 767–776.
- [49] D. Xu, W.D. Wu, H.-J. Qi, R.-X. Yang, W.-Q. Deng, Sulfur rich microporous polymer enables rapid and efficient removal of mercury(II) from water, *Chemosphere*, 196 (2018) 174–181.
- [50] J. Sun, H. Chen, D. Qi, H. Wu, C. Zhou, H. Yang, Enhanced immobilization of mercury (II) from desulphurization wastewater by EDTA functionalized graphene oxide nanoparticles, *Environ. Technol.*, 41 (2020) 1366–1379.
- [51] T. Javed, N. Khalid, N. Sareecha, M.L. Mirza, Sorption profile of mercury(II) from aqueous solution onto low-rank Pakistani coal, *Desal. Water Treat.*, 160 (2019) 276–287.
- [52] D.Z. Husein, Adsorption and removal of mercury ions from aqueous solution using raw and chemically modified Egyptian mandarin peel, *Desal. Water Treat.*, 51 (2013) 6761–6769.
- [53] A. Ates, E. Altintig, H. Demirel, M. Yilmaz, Comparative study on adsorptive removal of Cu, Pb, Zn heavy metals by modified perlite composites, *Desal. Water Treat.*, 98 (2017) 244–253.
- [54] S. Jafarnejad, M. Faraji, P. Jafari, J. Mokhtari-Aliabad, Removal of lead ions from aqueous solutions using novel-modified magnetic nanoparticles: optimization, isotherm, and kinetics studies, *Desal. Water Treat.*, 92 (2017) 267–274.
- [55] M. Candan, F. Tay, I. Avan, T. Tay, Removal of copper(II) and nickel(II) ions from aqueous solution using non-living lichen *Ramalina fraxinea* biomass: investigation of kinetics and sorption isotherms, *Desal. Water Treat.*, 75 (2017) 148–157.
- [56] K.F. Lam, K.L. Yeung, G. McKay, A rational approach in the design of selective mesoporous adsorbents. *Langmuir*, 22 (2006) 9632–9641.
- [57] A. Ma, T.H. Shek, S.J. Allen, V.K.C. Lee, G. McKay, Removal of nickel from effluents by chelating ion exchange, *J. Chem. Technol. Biotechnol.*, 83 (2008) 1623–1632.
- [58] P. Hadi, N. Chao, W. Ouyang, M. Xu, C.S.K. Lin, G. McKay, Towards environmentally-benign utilization of nonmetallic fraction of waste printed circuit boards as modifier and precursor, *Waste Manage.*, 35 (2015) 236–246.